Dev Genes Evol (2006) 216: 265–276
DOI 10.1007/s00427-005-0051-6

ORIGINAL ARTICLE

Taku Hibino · Yuichiro Ishii · Michael Levin · Atsuo Nishino

Ion flow regulates left–right asymmetry in sea urchin development

Received: 6 August 2005 / Accepted: 6 December 2005 / Published online: 14 March 2006

Abstract The degree of conservation among phyla of early mechanisms that pattern the left–right (LR) axis is poorly understood. Larvae of sea urchins exhibit consistently oriented LR asymmetry. The main part of the adult rudiment is formed from the left coelomic sac of larvae, the left hydrocoel. Although this left preference is conserved among all echinoderm larvae, its mechanism is largely not understood. Using two marker genes, *HpNot* and *HpFoxFQ-like*, which are asymmetrically expressed during larval development of the sea urchin *Hemicentrotus pulcherrimus*, we examined in this study the possibility that the recently discovered ion flux mechanism controls asymmetry in sea urchins as it does in several vertebrate species. Several ion-transporter inhibitors were screened for the ability to alter the expression of the asymmetric marker genes. Blockers of the H^+/K^+-ATPase (omeprazole, lansoprazole and SCH28080), as well as a calcium ionophore (A23187), significantly altered the normal sidedness of asymmetric gene expression. Exposure to omeprazole disrupted the consistent asymmetry of adult rudiment formation in larvae. Immuno-detection revealed that H^+/K^+-ATPase-like antigens in sea urchin embryos were present through blastula stage and exhibited a striking asymmetry being present in a single blastomere in 32-cell embryos. These results suggest that, as in vertebrates, endogenous spatially-regulated early transport of H^+ and/or K^+, and also of Ca^{2+}, functions in the establishment of LR asymmetry in sea urchin development.

Keywords Ion flux · Left–right asymmetry · Sea urchin · Embryogenesis · Adult rudiment

Communicated by N. Satoh

Electronic Supplementary Material Supplemantary material is available for this article at http://dx.doi.org/10.1007/s00427-005-0051-6

T. Hibino
Department of Biological Sciences,
Graduate School of Science, University of Tokyo,
Bunkyo-ku, Tokyo 113-0033, Japan

Y. Ishii · A. Nishino
Department of Integrated Biosciences,
Graduate School of Frontier Sciences,
University of Tokyo,
Kashiwa, Chiba 277-8562, Japan

M. Levin
Department of Cytokine Biology, The Forsyth Institute,
and Department of Developmental and Craniofacial Biology,
Harvard School of Dental Medicine,
140 The Fenway, Boston, MA 02115, USA

T. Hibino
Misaki Marine Biological Station, Graduate School of Science,
University of Tokyo,
Koajiro 1024, Misaki,
Miura 238-0225, Japan

T. Hibino
Division of Molecular and Cell Biology,
Sunnybrook and Women's College Health Sciences Centre,
Room S123A, 2075 Bayview Avenue,
Toronto, ON M4N 3M5, Canada

A. Nishino (✉)
Section for Developmental Neurophysiology,
Okazaki Institute for Integrative Bioscience,
Okazaki, Aichi 444-8787, Japan
e-mail: anishino@nips.ac.jp
Tel.: +81-56459-5258
Fax: +81-56459-5259

Introduction

Consistent asymmetries of organs, such as the heart and viscera, are overlaid upon the bilateral architecture of many animal phyla. Molecular mechanisms which establish LR asymmetry have been intensively investigated in vertebrate model organisms (Hamada et al. 2002; Mercola 2003; Cooke 2004; Levin 2005). Recent studies revealed a conserved regulatory cascade where a TGF-β factor, Nodal, is expressed in the left lateral mesoderm and positively controls the expression of the *Pitx2* gene, which functions to place the visceral organs with precise orientation (Ryan et al. 1998). However, the initial step for breaking the LR

symmetry and early mechanisms that establish consistently asymmetric gene expression are less well-understood. One model, based on data in rodent embryos, proposes that monocilia located in the node beat to propel the fluid containing possible determinant(s) to direct it to the left side (Nonaka et al. 1998, 2002; Tanaka et al. 2005); it has also been proposed that mechano-sensitive cells flanking the region of motile cilia sense the flow leading to an asymmetric calcium signaling (McGrath et al. 2003). While a comparable mechanism was reported in fish (Kramer-Zucker et al. 2005; Okada et al. 2005), data from other vertebrate models, the frog and chick, have suggested alternative mechanisms upstream of asymmetric gene expressions (Levin and Nascone 1997; Levin 2003, 2004a). Levin et al. demonstrated that a side-specific membrane hyperpolarization produced by the localized activity of the H^+/K^+-ATPase (H,K-ATPase) plays a critical role in LR patterning (Levin et al. 2002). This mechanism may control downstream events either through directly regulating signaling steps by altering steady-state membrane voltage levels, or by using the induced electrophoretic force to move as yet unidentified determinant(s) to a specific location around the midline. Another recent study suggested that Notch signaling is activated through a localized elevation of extracellular calcium concentration induced by a side-specific activity of H,K-ATPase (Raya et al. 2004). The degree of evolutionary conservation of these mechanisms among phyla, and their relevance in invertebrates, are an important current controversy (Boorman and Shimeld 2002; Cooke 2004).

Echinoderms, marine invertebrates including sea urchins and other pentameral organisms, show conspicuous LR asymmetry during their development. Most species initially develop from eggs into apparently bilateral planktotrophic larvae, and later metamorphose into five-rayed spiny-skinned adults (Peterson et al. 2000). During the late larval stage, a rudiment of the adult body is formed specifically on the left side of the larva. In sea urchins, the adult rudiment is differentiated from a left coelomic sac and the vestibular ectoderm; the former originates from the left mesodermal pouch pinched off from the archenteron tip, and the latter is derived from an invagination of a part of the oral ectoderm. The determination mechanisms have become clearer at a molecular level for the primary (animal–vegetal or anterior–posterior) axis (Logan et al. 1999; Weitzel et al. 2004), and also for the oral–aboral axis (Coffman et al. 2004; Duboc et al. 2004). The mechanism establishing asymmetry along the third axis, the LR axis, however, remains to be understood. Recently, a series of manipulation experiments in sea urchin embryos demonstrated that the ability to form the left adult rudiment is committed from gastrula to prism stages by an influence directed by a restricted part of the right side (Aihara and Amemiya 2000, 2001).

In this study, we address the molecular basis for this mechanism and characterize a novel aspect of LR asymmetry in sea urchin development. To test the hypothesis that ion flux is involved in breakage of LR symmetry of echinoid embryos, we performed a pharmacological screen using a set of compounds that modulate ionic flow (Adams and Levin 2005). Blockers of H,K-ATPase activity and a calcium ionophore significantly destabilized the normal LR asymmetry of the expression patterns of two molecular markers (as reported in abstract form in Ishii et al. 2003). Guided by these data, we characterized the localization of the H,K-ATPase in early sea urchin embryos, which revealed a strikingly asymmetric pattern at the protein level, revealing a deep similarity to early localization in vertebrates. Our analyses suggest that, as in chick and frog (Levin et al. 2002; Raya et al. 2004), an asymmetrically localized regulation of ion flux involving H^+ and/or K^+ is established from early embryonic stages and has an essential role for breakage of LR symmetry; moreover, the precise control of calcium flux is also required for determining asymmetry. Our results on endogenous localization and loss of function, together with the very recent finding (Duboc et al. 2005) that asymmetry can also be disrupted with an H,K-ATPase inhibitor in a Mediterranean sea urchin, *Paracentrotus lividus*, suggest that the early ion flux-dependent mechanism in LR patterning operates widely in echinoid lineage (Ishii et al. 2003; Duboc et al. 2005).

Materials and methods

Animals and embryos

Adults of the Japanese sea urchin, *Hemicentrotus pulcherrimus*, were collected at rocky shores in Ooarai (Ibaraki, Japan), Asamushi (Aomori, Japan), and Tateyama (Chiba, Japan). Eggs and sperm were obtained by injection of 100-mM acetylcholine chloride in the artificial seawater ("Jamarin U" artificial seawater, JSW, Jamarin Laboratory, Osaka, Japan) into the body cavity. After washes with JSW, eggs were inseminated with suspended sperm.

Pharmacological screening

Each compound (listed in Table 1) was dissolved in JSW, in which fertilized eggs were then reared to two-armed pluteus stage at about 18°C. We first prepared a series with graded concentrations for determining the appropriate concentration. While the batches displayed a variable response, we were able to define an appropriate concentration range for each compound at which the dissolved chemical did not disrupt the normal appearance of development until two-armed pluteus stage; the larvae retained a bilateral configuration with a well-shaped gut and skeletal rods (Table 1). It has been reported that treatment with A23187 is able to induce the formation of right-sided or bilateral adult rudiments (Fujiwara et al. 1997), and its treatment at a high dose, 2 μM, can also

Table 1 The compounds utilized in the present study

Compound	Concentration[a]	Expected target
A23187	60–120 nM	Calcium signaling
Amiloride Hydrochloride	100–150 μM	Na^+/H^+ exchanger
9-Anthracenecarboxylic Acid	135–270 μM	Cl^- channel
18α-Glycyrrhetinic Acid	50–100 μM	Gap junctions
Lansoprazole	25–50 μM	H^+/K^+-ATPase
Lanthanum Chloride Heptahydrate	100–200 μM	Ca^{2+} channel
Omeprazole	25–60 μM	H^+/K^+-ATPase
SCH28080	25–50 μM	H^+/K^+-ATPase

[a]Appropriate ranges of concentration to treat each with preventing apparent disorders along animal–vegetal axis and oral–aboral axis (see Materials and methods for more detail)

disrupt the oral–aboral axis specification and produce exogastrulae at a high incidence (Akasaka et al. 1997). We selected a dose for this compound that does not disrupt the normal gastrulation pattern (Table 1), and the exogastrulae formed occasionally were excluded from the further analyses. The normal specification of oral–aboral territories was confirmed by stomodeum development and the oral-sided expression of *HpNot*. This treatment disrupted the normally consistent sidedness of gene expression patterns at concentrations comparable to, and not more than fivefold greater than, those used in vertebrate experiments (see Results) (Toyoizumi et al. 1997; Levin et al. 2002; Asano et al. 2004). In each case, the final concentration level of DMSO (used as vehicle for compounds other than lanthanum chloride due to their insolubility directly into water) was less than 0.4%. Statistical analysis was performed using the *chi*-squared test. The numbers of larvae with particular gene expression pattern shown in Fig. 2 were calculated to determine *p* values. The 2×2 matrices were prepared from the numbers of larvae retaining the normal side-specificity (namely, R and TR patterns for *HpNot* expression in Fig. 2C) and larvae with other patterns from each treatment vs those from the negative control. Negative control embryos for lanthanum chloride were exposed to JSW only, while 1% DMSO treatment was used as a negative control treatment for the other compounds.

To examine the side-specificity of adult rudiment formation, treated larvae were reared according to the method described (Amemiya 1996), within 50-ml plastic tubes containing JSW (~60 larvae/50 ml) fixed on a rotator for 2 weeks. They were fed with cultured diatoms, *Chaetoceros gracilis* and/or *C. calcitrans* (the latter is commercially supplied as "sunculture", Nisshin Marinetech, Yokohama, Japan). The growth of larvae was examined once every 3 days, and after the examination the larvae were transferred into a new suspension of diatoms. The larvae aged up to eight-armed pluteus after 2 weeks were observed under a binocular dissection microscope to determine the side on which adult rudiment formed. Sometimes, vestibular invagination was found without any evident adult organs derived from the coelom. In such cases, the side of the vestibule was assessed and categorized into 'L (or R) vestibule only'. For statistics, a *chi*-squared test was performed with the counts of larvae with normal side specificity (namely, L and l.v. patterns) and larvae with other patterns. Larvae were photographed from the aboral side under a light microscope (Fig. 3).

Alkaline phosphatase histochemistry

The expression of alkaline phosphatase (APase) histoactivity has been regarded as a differentiation marker for the endoderm of echinoid larvae. The expression of APase is known to start in *H. pulcherrimus* about 30 h of postfertilization (hpf) at 18°C (Hamada and Kiyomoto 2003). The omeprazole treated and non-treated prism larvae at 30.5, 32.5, 34.5, and 36.5 hpf were fixed by 4% paraformaldehyde in 0.1 M MOPS (pH 7.5), 0.5 M NaCl for 10 min at room temperature, followed by several washes with APase buffer (100 mM Tris–Cl pH 9.5, 100 mM NaCl, 5 mM $MgCl_2$). The fixed larvae were stained by adding 20 μl/ml nitroblue tetrazolium/bromo-chloro-indolyl phosphate (NBT/BCIP) stock solution (supplied in DIG DNA labeling and detection kit, Roche) in APase buffer for 30 min in the dark at room temperature. The coloring reaction was stopped by a wash with PBT (phosphate buffered saline containing 0.1% Tween-20). The stained larvae were photographed under a light microscope (Axioplan 2, Zeiss) and a digital photo system (DC300FX, Leica) with constant digital parameters. The incorporated RGB color images were converted into 8-bit gray-scale pict files by Photoshop 7.0, and then analyzed using NIH image 1.63 run on a G3 Macintosh computer. The region of interest (ROI) was defined to include the gut region of a randomly selected larva, and the maximum pixel value (at most, 255=black) in the ROI was taken to represent the APase expression level. The average of the values from 20 individuals was defined as "APase expression index", and the indices were compared with samples from different sampling stages and different treatment conditions (see Supplementary Fig. S1).

Whole-mount in situ hybridization

H. pulcherrimus gastrulae and larvae were fixed in 4% paraformaldehyde in 100 mM MOPS (pH 7.5), 0.5 M NaCl for overnight at 4°C. Whole-mount in situ hybridization was performed essentially as described (Arenas-Mena et al. 2000). The stained specimens were photographed using a digital photo system (SPOT, Diagnostic Instruments) with a light microscope (Power BX, Olympus). The LR directions of the stained larvae were carefully determined

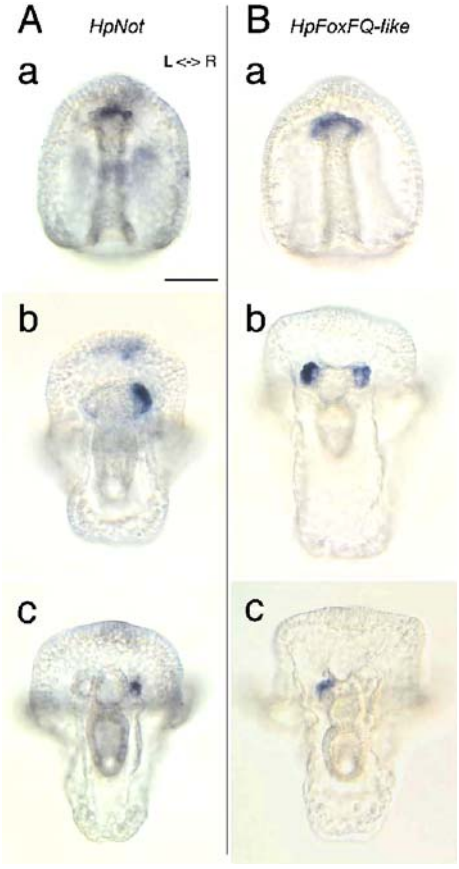

Fig. 1 Establishment of LR asymmetrical gene expression during prism-pluteus stage. **A** Right-sided expression of *HpNot* transcript. The transcript is found at the top of archenteron in prism stage (**a**, 27 hpf). The signal at the archenteron tip is incorporated into the right forming coelomic sac (**b**, 36 hpf, two-armed pluteus). The *HpNot* signal is fully segregated in the right coelom of late two-armed pluteus (**c**, 42 hpf). Scale bar in *a*=50 μm for all panels. **B** Left-sided expression of *HpFoxFQ-like* transcript. In prism stage, the transcript is localized at the archenteron tip, and the expression domain starts divided into the left and right populations (**a**, 30 hpf). Those populations are segregated into the left and right coelomic sacs of two-armed pluteus larva (**b**, 38 hpf), where the left population always exhibits more intense signal than the right one. In late two-armed pluteus (**c**, 42 hpf), the left coelom remains to express *HpFoxFQ-like*, while the signal in the right has disappeared. All the panels show aboral view of larvae

under the microscope, based on the positions of oral-sided bilateral clusters of primary mesenchyme cells in gastrulae and prisms, and of bilateral arms and oral hood in plutei.

Immunohistochemistry

For the fixation of embryos before hatching stages, eggs were inseminated in JSW containing 1 mM aminotriazole to prevent hardening of the fertilization envelope, and the formed envelopes were removed by gentle pipetting (Showman and Foerder 1979). The collected embryos and larvae were fixed with 2% paraformaldehyde in 0.1 M MOPS (pH 7.5) and 0.5 M NaCl for 30 min at room temperature. The fixed specimens were extracted with cold methanol for 5 min and transferred into 70% ethanol. The specimens were stored in 70% ethanol at −20°C or in PBT containing 0.1% NaN_3 at 4°C. Some specimens were embedded in gelatin/albumin as described (Levin 2004b). The blocks were sectioned at 20 μm and processed for immunohistochemistry using standard methods. Sections were blocked with PBT-BSA (PBT with 1% bovine serum albumin) plus 10% goat serum. An antibody for *Xenopus* H,K-ATPase α- or β-subunit (kindly provided by Dr. Kaethi Geering) was used at a 1:500 dilution, followed by PBS-BSA washes (six times, 1 h each). An APase-conjugated anti-rabbit secondary antibody was applied at a dilution of 1:1,500, followed by washes (six times, 1 h each), and detected using the standard BCIP/NBT substrate.

Western blotting

Blastula-stage embryos were rapidly frozen in the −80°C freezer and resuspended in lysis buffer (TritonX-100, 50 mM NaCl, 10 mM NaF, 1 mM Na_3VO_4, 5 mM EDTA, 10 mM Tris–Cl pH 7.6, 2 mM PMSF). Protein solution was mixed at 1:1 with Laemmli sample buffer (BioRad) containing 2.5% 2-mercaptoethanol. The proteins were fractionated by SDS-PAGE and electrotransferred to a PVDF membrane. After washing, the membrane was blocked with 3% BSA and 5% dry milk in Tris-buffered saline including 0.1% Tween-20 (TTBS). It was then incubated overnight in a Mini-PROTEAN II multiscreen appatus (BioRad) at 4°C with the primary antibody to *Xenopus* H,K-ATPase β-subunit, diluted in TTBS plus 3% BSA and 5% dry milk (1:3,000). After washing, the blots were incubated with peroxidase-conjugated secondary antibody (1:5,000) in the same buffer and developed using an ImmunoStar Chemiluminescent Protein Detection System (BioRad) according to the manufacturer's instructions.

Results

HpNot and *HpFoxFQ-like* exhibit distinct LR asymmetrical expression in prism-pluteus stage

We recently found that the *Not*-type homeobox gene ortholog of *H. pulcherrimus*, *HpNot* (DDBJ accession no. AB183890), is expressed in the right coelomic pouch, but not in the left, of two-armed pluteus larvae (Fig. 1A; the detailed expression pattern throughout embryogenesis will be reported elsewhere). The asymmetric localization of the transcript began at prism stage at the tip of archenteron (Fig. 1Aa). The signal at the archenteron tip moved into the right pouch of bilaterally forming coela, and finally in a two-armed pluteus stage at 42 hpf; the mesodermal expression was restricted to the right coelom, but not to the left (Fig. 1Ab,c).

Spfoxc was reported as an expressed sequence tag in another sea urchin *Strogylocentrotus purpuratus*, which

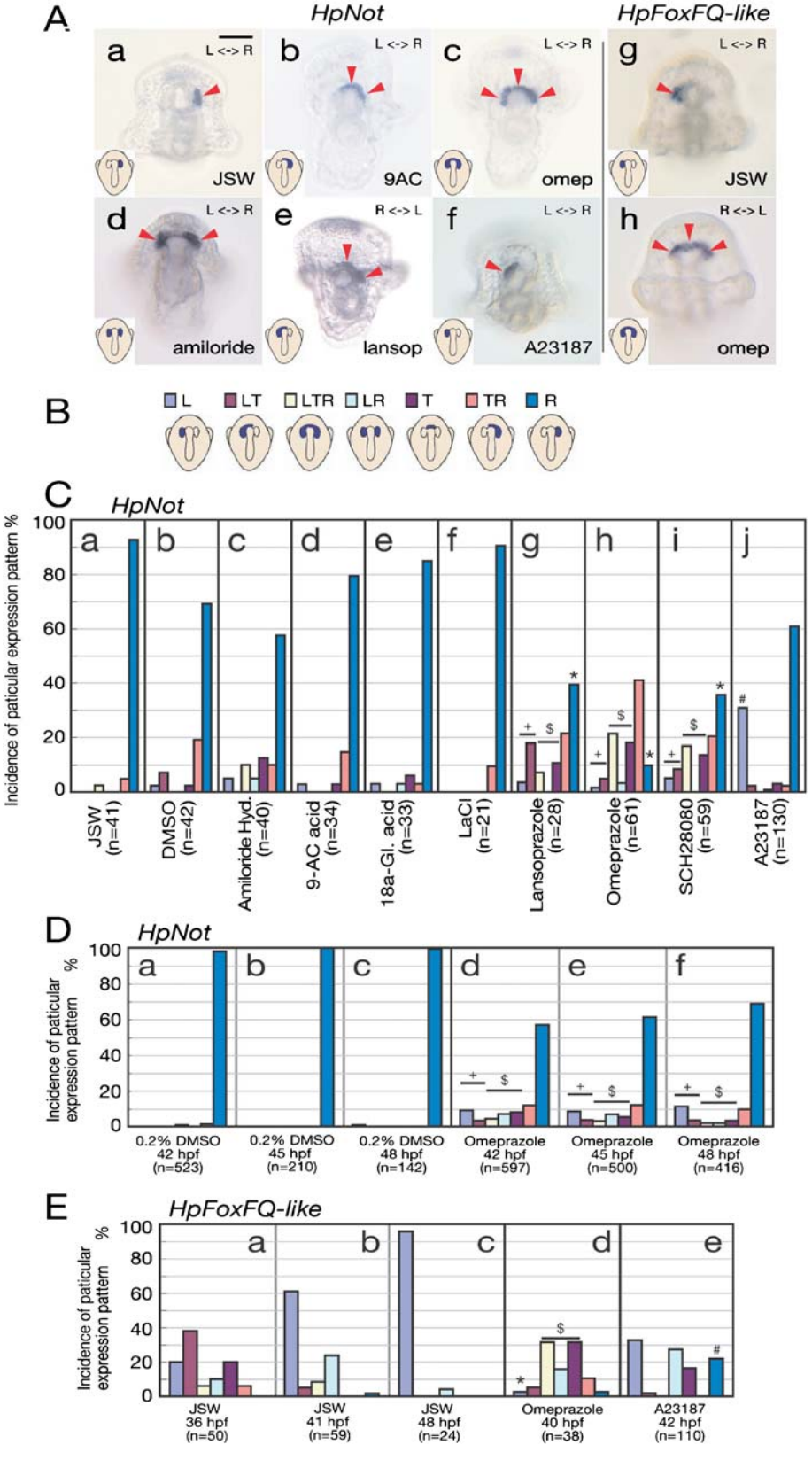

Fig. 2 H,K-ATPase blockers and a calcium ionophore affect the expression pattern of LR asymmetry genes. **A** The patterns of disrupted *HpNot* and *HpFoxFQ-like* expression around the archenteron tip were classified into seven categories. The representative patterns are shown (**a**–**h**). The larvae had been exposed after fertilization to the reagent noted in each panel as below; JSW, normal seawater; 9AC, 9-anthracenecarboxylic acid; omep, omeprazole; lansop, lansoprazole. After fixation at 40–42 hpf in two-armed pluteus stage, gene expression of *HpNot* (**a**–**f**) and *HpFoxFQ-like* (**g**, **h**) was assessed by in situ hybridization. Note that the treatments do not disturb the anterior–posterior or oral–aboral axis specification at the doses indicated in Table 1. Panels e and h show the oral view, while others show the aboral view. Schematic illustrations of expression sites are provided in each panel. Bar=50 μm. **B** The seven categories of signal distribution pattern. *L*: left-side specific, *LT*: signals at left-side pouch as well as just above the archenteron tip, *LTR*: covering tip of archenteron from left to right, and so on. Each category is labeled by a color, that is consistently used in the graphs below **C**, **D**, **E**. **C** The effect of compound treatment for *HpNot* expression patterns. **D** Evaluation of the effect of omeprazole in larger populations. Panels a–c and d–f show incidences of each *HpNot* expression pattern in negative control (0.2% DMSO only) populations and 58 M omeprazole-treated populations, respectively, that were sampled from three stages; two-armed pluteus stage (42 hpf) and early four-armed pluteus stages (45 and 48 hpf). **E** The effect of compound treatment on *HpFoxFQ-like* expression pattern (**d**, **e**). Panels a–c show transitions of *HpFoxFQ-like* expression pattern during early to late two-armed pluteus stages. The *asterisks* mark the decrease of normal pattern derived from the H,K-ATPase blockers, and + and $ mark the increase of reversed and bilateral patters, respectively. The high incidence of reversed patter by A23187 is highlighted with #

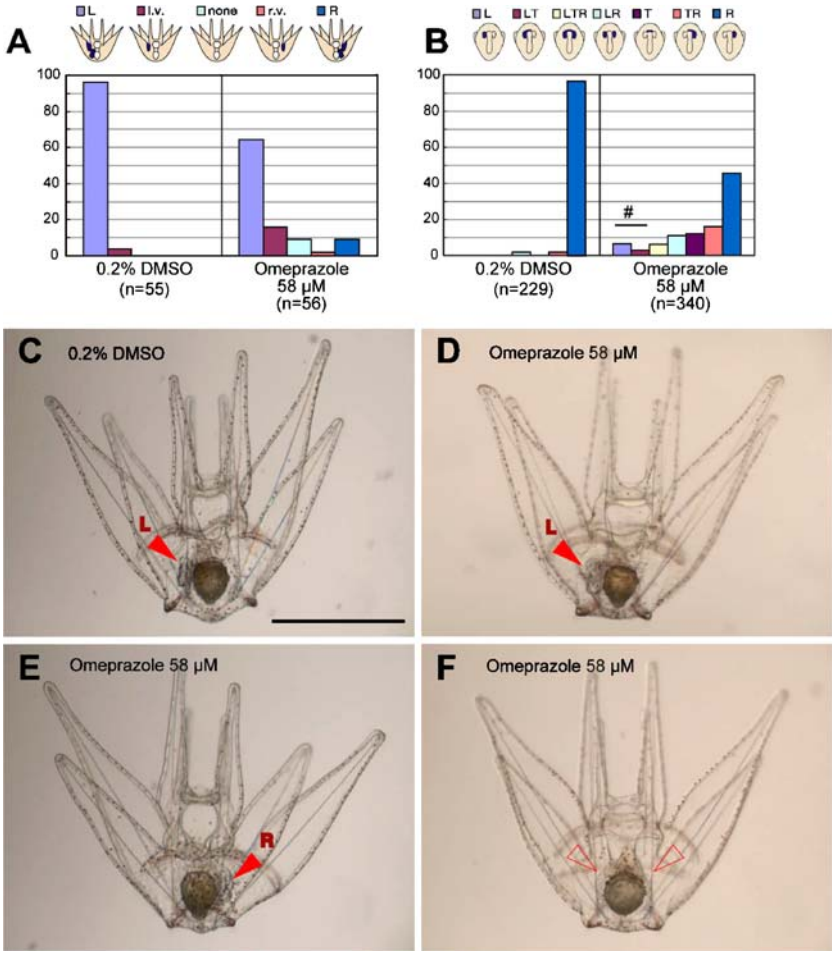

Fig. 3 Omeprazole disrupts the consistently asymmetric formation of the adult rudiment. **A**, **B** Effect of omeprazole treatment (up to 40 hpf, two-armed pluteus stage) on the placement of adult rudiment in eight-armed plutei (**A**), and on the expression pattern of *HpNot* (**B**) to the population from the identical batch. Although many of the treated larvae exhibited normal left positioning of the rudiment, some larvae formed a rudiment on the right and others showed no sign of adult rudiment formation (**A**). A comparable incidence was found between the reversed adult rudiment in eight-armed pluteus stage (**A**) and the reversed *HpNot* expression (**B**, #). **C** Normal eight-armed pluteus containing adult rudiment in the left half of the body. This individual is derived from the population treated with the solvent only (0.2% DMSO). **D, E, F** Eight-armed plutei derived from the population treated with 58 µM omeprazole. The left (normal) rudiment (**D**) and right (inversely placed) rudiment (**E**) are indicated with *arrowheads*. The absence of evidence of rudiment formation is indicated by *open arrowheads* (**F**). All the panels show aboral view of eight-armed plutei (about 2 weeks after fertilization). Bar=500 µm

showed a LR asymmetric expression pattern (Ransick et al. 2002). We cloned a closely related cDNA from *H. pulcherrimus*, which contained a full coding sequence, and named *HpFoxFQ-like* (DDBJ accession no. AB 191390). The expression pattern of this transcript in *H. pulcherrimus* prism-pluteus larvae was quite similar to that described on *Spfoxc* (Ransick et al. 2002). In short, the *HpFoxFQ-like* transcript was found at the top of the differentiating gut of prisms (Fig. 1Ba). At 38 hpf, the two-armed pluteus stage, the signal at the archenteron tip, was divided and incorporated into the coelomic sacs. At that time, the left-sided signal was always with more intensity than the right one (Fig. 1Bb). Two-armed plutei at 42 hpf showed specific expression in the left coelomic pouch, while the right one ceased to express the signal (Fig. 1Bc). These clearly show that *HpNot* and *HpFoxFQ-like* can be used as right and left-specific asymmetric gene markers, respectively.

A pharmacological screen implicates ion flux upstream of *HpNot* expression

Using these markers, we sought to examine whether, as recently reported in vertebrates (Levin et al. 2002; Raya et al. 2004), ion flux was required for the correct sidedness of asymmetric gene expression. To test this and to identify candidate electrogenic genes for subsequent analysis (Adams and Levin 2005), we utilized a number of well-characterized drug blockers targeting plasma membrane ion flow or gap-junctional communication (Table 1). Those compounds were applied continuously after fertilization,

and two-armed plutei at 40–42 hpf were fixed for analysis by in situ hybridization against *HpNot*. The expression patterns of *HpNot* varied considerably among treated individuals, and we categorized the expression patterns seen at the archenteron tip and coelomic pouches into seven classes (Fig. 2A,B). Larvae developed in the artificial seawater (JSW) showed a 90% incidence of normal right side-specific expression (Fig. 2Aa,Ca). Exposure to 1% DMSO, a common vehicle, decreased the right-specific pattern to 70%, but the majority of the rest showed the top-right (TR) pattern; namely, they retained the right-sided pattern (Fig. 2Cb); $p \approx 0.096$ for JSW vs 1% DMSO). Thus, DMSO was used at final concentration of 0.4% or less for analyses below, a level that does not affect the right-sided pattern of *HpNot*. Most of the candidate compounds tested were found not to have significant effects on LR-asymmetric expression of *HpNot*; these included amiloride hydrochloride (DuVall et al. 1998; Harris and Fliegel 1999), 9-anthracenecarboxylic acid (Landry et al. 1987), 18α-glycyrrhetinic acid (Davidson and Baumgarten 1988), and lanthanum chloride (Nathan et al. 1988) (Fig. 2Cc,e,f); $p > 0.02$, 0.36, 0.97, and 0.47, respectively; see Materials and methods for the calculation). Based on these data, we conclude that amiloride-sensitive Na^+ channels, the Na^+/H^+-ATPase, Cl^- channels, Ca^{2+} channels, and gap-junctional communication are not required for the asymmetric expression of *HpNot*. Importantly, these data indicate that LR asymmetry in sea urchins is not labile, and is not generally sensitive to non-specific pharmacological perturbation.

In contrast, treatment with lansoprazole, a member of a class of blockers which specifically inhibit the H,K-ATPase pump in organisms ranging from protozoa to mammals (Sanders et al. 1992; Jiang et al. 2002), significantly randomized the normal *HpNot* pattern ($p < 0.008$; Fig. 2Cg, asterisk). This observation raised the possibility that endogenous H,K-ATPase activity may function in the patterning of the LR axis in echinoid development. To further test the possibility that the H,K-ATPase is a component of the mechanisms upstream of LR asymmetric gene expression, we examined the effects of other specific blockers of the H,K-ATPase, omeprazole (Sachs et al. 1995) and SCH28080 (Munson et al. 2000). Both of these compounds also destabilized significantly the normal expression pattern of *HpNot* (Fig. 2Ch,i; asterisks; $p < 10^{-4}$, 10^{-3}, respectively). A considerable number of larvae treated with lansoprazole, omeprazole, or SCH28080 exhibited bilateral expression (LTR, LR and T patterns, marked with $ in Fig. 2Cg–i), and also did reversed expression (L and LT patterns, marked with +).

General developmental delay could possibly be caused by treatment of the compounds. The alkaline phosphatase (APase) expression levels were examined to determine if omeprazole treatment resulted in delay of endomesodermal tissue development. In treated embryos, weak expression of APase activity was found in the gut of 30.5 hpf prisms, and then the signal intensity increased in following 6 h (Supplementary Fig. S1); this time course was quite consistent with that in the control embryos, as well as a previous report (Hamada and Kiyomoto 2003). The paired coelomic pouches were also well-formed in larvae exposed to omeprazole. Therefore, we conclude that developmental delay is insignificant and cannot explain the increase of the bilateral expression patterns.

To assess further the effect of omeprazole on the sided *HpNot* expression, a large number of the omeprazole-treated and non-treated larvae were examined at 42, 45, and 48 hpf (Fig. 2D). While most larvae in the control population (98%) established right-side specific *HpNot* by 42 hpf (Fig. 2Da–c), incidence of the normal right specific pattern was decreased to 57% (42 hpf) ~ 69% (48 hpf) in the population exposed to 58 μM omeprazole (Fig. 2Dd–f). Increases of both reversed and bilateral patterns were observed (Fig. 2Dd–f; + and $, respectively), being consistent with the results from smaller populations, described above (Fig. 2Cg–i). During 6 h from 42 hpf, incidence of bilateral patterns decreased, and those of normal and reversed patterns slightly increased (Fig. 2Dd–f). The disruption of sided *HpNot* expression was statistically supported by *chi*-squared tests ($p < 10^{-8}$ in every stage).

Another compound with a significant effect on laterality was the calcium ionophore, A23187. Treatment with A23187 disrupted the normal pattern ($p < 0.003$), causing a dramatic increase in the incidence of the inverted expression pattern (L pattern) (Fig. 2A,Cj, #). These data show that a significant incidence of LR defects in the sidedness of *HpNot* expression can be caused by H,K-ATPase blockers, and also by a calcium ionophore.

The H,K-ATPase blocker and the calcium ionophore disrupt the normal asymmetric localization of *HpFoxFQ-like*

HpNot is a right-side marker, while *HpFoxFQ-like* is expressed preferentially in the left coelom (Fig. 1). We asked whether, like *HpNot*, the laterality of the left-sided gene is also affected by the exposure of the H,K-ATPase blockers and the calcium ionophore. Omeprazole and A23187 were continuously applied after fertilization, and the expression patterns of *HpFoxFQ-like* were analyzed in the 40–42 hpf two-armed plutei (Fig. 2E). A significant number of normal larvae exhibited signal in both sides of coelomic pouches during the growth of two-armed plutei (Fig. 2Ea–c). This complicated pattern made it more difficult to assess the effect of the compounds than when *HpNot* was used as a marker. However, a considerable decrease of left-directed expression (Fig. 2Ed, asterisk) and increases of bilateral patterns (Fig. 2Ed, $) were observed in omeprazole-treated larvae. A23187 treatment induced a 22% incidence of the reverse-sided expression of *HpFoxFQ-like* (Fig. 2Ee, marked with #). These data suggest that the LR asymmetric pattern of *HpFoxFQ-like* expression is likewise affected by the H,K-ATPase blocker and the calcium ionophore.

Omeprazole can disrupt the side-specificity for the adult rudiment placement

Sea urchin larvae consistently form the adult rudiment on the left side of the body in six- to eight-armed pluteus stage. It was already known that A23187 has the ability to disorder the sided placement of adult rudiment (Fujiwara et al. 1997). To determine whether omeprazole can disrupt the left-side specific placement of the rudiment in the aged larvae, the omeprazole-treated two-armed plutei were reared for 2 weeks. All of the larvae untreated or exposed to 0.2% DMSO (the vehicle solvent) showed normal left rudiment. On the other hand, exposure to 58 μM omeprazole up to two-armed pluteus stage (0–40 hpf) brought about significant numbers of eight-armed larvae whose side-specific rudiment formation was disrupted (Fig. 3A; $p<10^{-4}$, see Materials and methods for the calculation). The inverted placement of adult rudiment was found in the treated population (Fig. 3A,E; about 11% in this shown case and 4% in the least case we encountered). Interestingly, some treated larvae showed no indications of the rudiment in spite of their well-shaped eight arms (Fig. 3A,F). More often, larvae exhibiting diminished rudiment formation were also found, where the vestibule, side-specific ectodermal invagination, was only detected without any signs of mesodermal transformation (l.v. and r.v. patterns in Fig. 3A). Such cases were seldom seen in the control populations (Fig. 3A). Sibling two-armed plutei, fixed previously from the same treated batch, showed a disruption pattern of *HpNot* expression ($p<10^{-23}$) and exhibited the comparable incidence (~10%) of reverse-sided expression of *HpNot* (Fig. 3B, marked with #).

H,K-ATPase-like immunoreactivity is specifically localized from cleavage to blastula stages

We performed immunohistochemistry on whole or sectioned embryos using polyclonal antibodies raised against the *Xenopus laevis* H,K-ATPase subunits. Western blot analysis using antibody for the β-subunit showed a single,

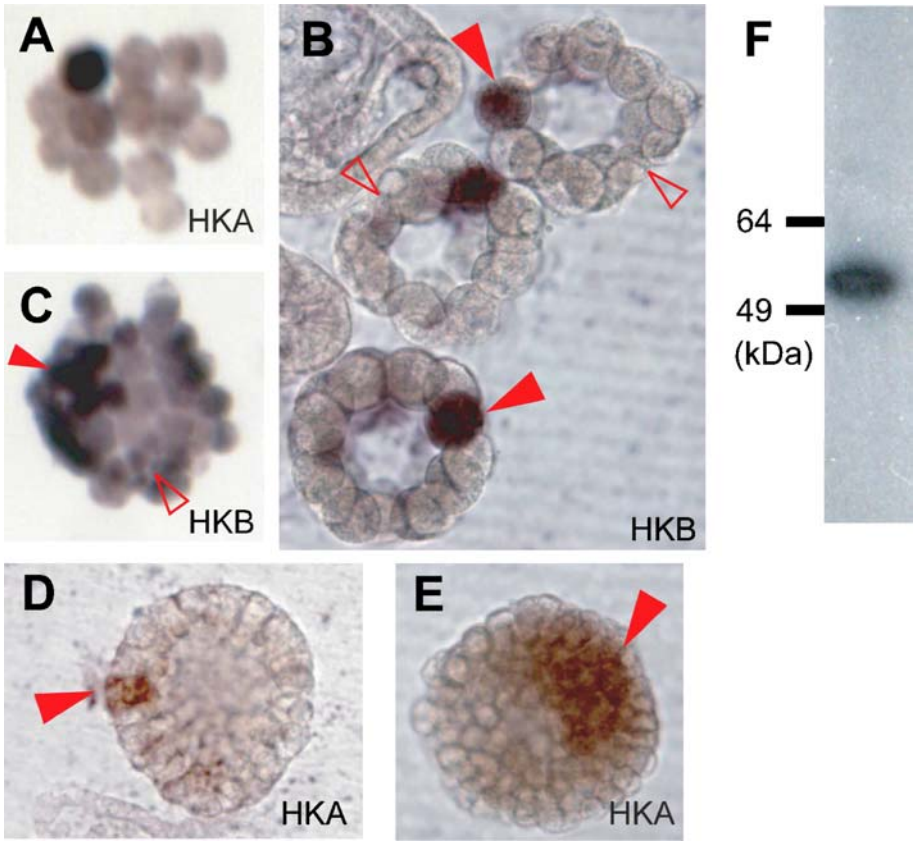

Fig. 4 The localization pattern of H,K-ATPase α- and β-subunit-like antigens during *H. pulcherrimus* development. **A** A localized expression of antigen is detected in a single blastomere of the early cleavage-staged embryo (*red arrowhead*) by a *Xenopus* H,K-ATPase α-subunit (HKA) antibody. This view shows a 32-cell stage embryo partly disaggregated during processing. **B** The H,K-ATPase β-subunit (HKB)-like antigen is expressed in a blastomere of 32-cell stage embryos. The positive cell seems located in the animal side, based on the probable position of micromere descendants (*open arrowheads*). The embryos were processed within a slice of gelatin (see Materials and methods). **C** Morula with a localized HKB antigen expression. **D, E** In blastula stage, some embryos showed HKA signal within a single cell, while others in multiple cells. The expressing territory is polarized in one side of embryo. These were processed in gelatin slices. **F** Western blot analysis by HKB antibody. The size of the single detected band (*arrow*) is estimated as about 52 kDa. For all panels, *arrowheads* indicate signals, and *open arrowheads* indicate the probable position of micromere descendants, namely, the vegetal pole region

strong, specific band, whose molecular weight (~52 kDa) was comparable with those of the vertebrate cognates (Fig. 4F). A strikingly asymmetric expression was detected; the antibodies to the α-subunit or the β-subunit of H,K-ATPase stained a single blastomere of 32-cell embryos (Fig. 4A,B). The blastomere occupied a radially asymmetrical location for embryos, which was determined by the direction of presumed animal–vegetal axis (Fig. 4B). Later, the positive cells were often more numerous and remained occupying a side of embryos through cleavage-blastula stages (Fig. 4C–E). No evident signal was found during gastrula stages (data not shown). These data reveal an established asymmetry in the sea urchin embryo at a very early stage and suggest that the target of the H,K-ATPase loss-of-function reagents used in our screen does indeed exist in the sea urchin embryos.

Discussion

The present study showed that H,K-ATPase blockers disrupted normal distribution of LR asymmetric gene expression sites and the placement of adult rudiment, and also revealed that the H,K-ATPase-like antigens are localized asymmetrically in the early embryos of the echinoid. These data extend prior observations suggesting involvement of the H,K-ATPase in asymmetry (Ishii et al. 2003; Duboc et al. 2005), and strongly implicate an H,K-ATPase-like protein as a crucial component of invertebrate LR patterning.

Breaking the radial/bilateral symmetries in early sea urchin embryogenesis

The H,K-ATPase is a member of P-type ATPase family, which also includes the Na,K-ATPase and sarcoplasmic reticulum Ca^{2+}-ATPase. They consist of α- and β-subunits, and the binding sites for ATP, H^+, and K^+ are all found in the α-subunit. The β-subunit contributes to the stabilization of the complex within the membrane (Møller et al. 1996). Omeprazole and lansoprazole are benzidazoles that can be stabilized and activated in an acidic environment to form a cationic sulfenamide. They are activated by the microenvironmental acidity created by H,K-ATPase and other ubiquitous H^+ pumps, and the derivative reacts with cysteine residues in the extracellular surface of the α-subunit to inhibit its catalytic activities. The specificity and resulting low incidence of side-effects have made these compounds useful clinical reagents (Vakil 2003). Another blocker, SCH28080, is an acid pump antagonist with a high specificity to gastric H,K-ATPase, targeting a site of the α-subunit that is partially overlapping to, but distinct from, the target site(s) of omeprazole (Asano et al. 2004). SCH28080 does not need acid-activation to block H,K-ATPase activity. These compounds are also known to be effective and specific blockers of protozoan H,K-ATPases (Mukherjee et al. 2001; Jiang et al. 2002), demonstrating the high applicability of these compounds as H,K-ATPase loss-of-function reagents for a wide variety of organisms. While *H,K-ATPase* genes have not been characterized in sea urchins to date, its functional existence in development has been suggested (Mitsunaga et al. 1987).

Three different H,K-ATPase inhibitors (comprising two different mechanisms of blockade) disrupted the sidedness of asymmetric markers at a statistically significant level at physiological concentrations. Importantly, consistent with the specificity of the H,K-ATPase inhibitors utilized in this study, a number of channel/pump inhibitors had no effect on asymmetry, indicating that asymmetry is not a highly labile process in the sea urchin, and that general pharmacological inhibition of ion flux is not sufficient to randomize it. Moreover, the treatments did not disturb the anterior–posterior or oral–aboral axis specification at the doses indicated in Table 1, making secondary effects on asymmetry (through simple toxicity) unlikely. This possible effect was also carefully excluded by histochemical test of APase expression (Supplementary Fig. S1). The treatment with H,K-ATPase blockers often induces a transposition of *HpNot* and *HpFoxFQ-like* signals around the archenteron tip region, from side-specific manner (R and TR pattern for *HpNot*, L and LT for *HpFoxFQ-like*) to reversed or bilateral patterns. The increase of LTR and reversed populations with those blockers also indicates that this phenotype is not a mere developmental delay but a true laterality defect. Considering that many larvae exhibited an incompleteness of allocation of expression sites into the pouch with associating increases of TR pattern in the *HpNot* case and of LT pattern in the *HpFoxFQ-like* case, the effect caused by H,K-ATPase blockers seems to reflect a 'weakened potential' to exert consistently biased differences between LR pouches (Fig. 2). Such a suppression of the potential would also be represented in the gradual decrease of bilateral patterns and increase of unilateral (polarized) patterns of *HpNot* observed during 6 h after 42 hpf in the omeprazole-treated larvae (Fig. 2D). It seems consistent with the frequent occurrence of the insufficient formation of adult rudiment in the treated population of eight-armed larvae (Fig. 3). These functional data are consistent with the model that sea urchin embryos utilize H^+ and/or K^+ gradient(s) evoked by an H,K-ATPase activity upstream of the expression of asymmetric genes in the LR pathway that finally leads to sided morphology of the larvae. The very recent report by Duboc et al. also demonstrated that the exposure of *P. lividus* embryos to 100 μM omeprazole for 0–48 hpf disrupts the side-specific expression of *Nodal* and *Sox9* genes, which is consistent with our results (Ishii et al. 2003; Duboc et al. 2005). However, prior reports did not examine the endogenous presence of H,K-ATPases in the embryo nor provided information on the distribution of such activity. Therefore, we used immunohistochemistry to show that these targets indeed exist in embryogenesis and acquire spatial information necessary for the formulation of models of the evolution of LR mechanisms across phyla.

The presence of an H,K-ATPase-like antigen with a radially asymmetrical pattern in the cleavage-stage embryo suggests that an H,K-ATPase protein targeted by the

blockers exists endogenously in embryos from very early stages of development. Importantly, although mitochondria and some mRNAs (COUP-TF and a collagen) exhibit graded localization in the egg and early embryo (Vlahou et al. 1996; Gambino et al. 1997), the discrete expression pattern of H,K-ATPase-like antigen is unique in its localization, and in that it suggests a novel mechanism to specify an early blastomere to establish the radial asymmetry. Extensive cell lineage tracking will be required to identify the exact location of the H,K-ATPase-positive blastomere along the LR or dorsoventral axis, but asymmetric localization of electrogenic proteins indicates that a patterning process that leads to the future LR asymmetry emerging weeks later has already occurred prior to the 32-cell stage.

Recent researches by Coffman et al. revealed that a redox gradient driven by maternally localized mitochondria contributes to specify the oral face (Coffman and Davidson 2001; Coffman et al. 2004). Physiological relationships between this reported redox gradient and the proposed H^+/K^+ gradient represent a promising avenue for understanding the linkage between the LR axis and the oral–aboral axis.

The phylogenetically conserved requirement of H^+/K^+ and Ca^{2+} ion flows for establishment of LR asymmetry

Besides the functional importance of H,K-ATPase in early development, the results obtained from A23187 treatment implicate calcium ion flow in LR determination. It was shown in vertebrates that a side-specific membrane hyperpolarization produced by the localized activity of the H,K-ATPase constitutes the early step for LR establishment, and that signaling steps involving side-specific calcium ion regulation are required in later stages (Toyoizumi et al. 1997; McGrath et al. 2003; Raya et al. 2004). In frog embryos, the required period for H^+ and K^+ flux to function in LR patterning is from early cleavage to blastula stages; the function can be blocked by omeprazole, lansoprazole, or SCH28080 (Levin et al. 2002). In chick, the period is from the initiation of the primitive streak to the time prior to the formation of Hensen's node (Levin et al. 2002; Raya et al. 2004). It is also known in *Xenopus* that the H,K-ATPase exhibits a side-specific enrichment from very early cleavage stage (Levin et al. 2002), which is paralleled for the early asymmetrical localization of H,K-ATPase-like antigens shown in this study in the sea urchin.

In contrast with H^+ and K^+ fluxes, Ca^{2+} appears to be involved a bit later in mouse and chick LR development, and during gastrulation and neurulation (McGrath et al. 2003; Raya et al. 2004). Similarly, in *Xenopus*, a calcium ionophore is known to induce 50% or more heterotaxia when applied during neurula stages (Toyoizumi et al. 1997). It was shown in chick that an extracellular Ca^{2+} gradient was established around the Hensen's node as a reflection of the precedent H,K-ATPase activity (Raya et al. 2004). Interestingly, while the vertebrate experiments suggest a role for Ca^{2+} signaling, they do not implicate a specific Ca^{2+} channel (Levin et al. 2002; McGrath et al. 2003; Raya et al. 2004). Our pharmacological data reveal no effect of a calcium channel blocker (lanthanum chloride) but a strong effect of a calcium ionophore. This may imply that the common role of calcium is mediated not by movement of the ion through Ca^{2+}-selective channels but by some Ca^{2+}-dependent cellular mechanism.

These parallel data sets suggest that precise regulations of ion flux during early developmental periods are a conserved mechanism upstream of asymmetric gene expression in a wide variety of deuterostomes, where the localized activity of H,K-ATPase, as well as calcium ion regulation, is a prerequisite for the correct sided expression of LR asymmetrical genes. Future work will be focused on characterization of endogenous ion flux and upstream mechanisms controlling H,K-ATPase asymmetry in sea urchin embryogenesis. These may provide a shared platform for highlighting a common early mechanism for the embryonic development of deuterostomes' chiral bodyplans.

Acknowledgements We are deeply grateful to Dr. Shonan Amemiya for supporting and encouraging us to progress this work in his laboratory. We thank Dayong Qiu for his critical assistance with the Western blotting, and Dr. Tetsuya Kominami and Dr. Shoji Oda for valuable discussions. Dr. Masaaki Yamaguchi provided the cDNA library. Dr. Kaethi Geering allowed us to use the antibodies for H,K-ATPase. The staff at Asamushi Marine Biological Station, Tohoku University provided ripe sea urchins. AN and TH are thankful to Dr. Yasushi Okamura in Okazaki Institute for Integrative Bioscience and Dr. Koji Akasaka in Misaki Marine Biological Station for the encouragement. AN was supported by Narishige Zoological Science Award in 2002, and by JSPS research fellowship (no. 2291) from 2004. This work had also been supported by a grant-in-aid from MEXT, Japan. ML gratefully acknowledges the support of the American Cancer Society (Research Scholar Grant RSG-02-046-01) and the National Institute of Health (1-R01-GM-06227). Part of this investigation was conducted in a Forsyth Institute facility renovated with support from Research Facilities Improvement Grant Number CO6RR11244 from the National Center for Research Resources, National Institutes of Health.

References

Adams D, Levin M (2005) Ion fluxes and gap junctional communication: probing biophysical epigenetic factors in *Xenopus* patterning. In: Whitman M and Sater AK (eds) Analysis of growth factor signaling in embryos (Methods in Signal Transduction Series). CRC (in press)

Aihara M, Amemiya S (2000) Microsurgery to induce formation of double adult rudiments in sea urchin larvae. Invert Reprod Dev 37:241–248

Aihara M, Amemiya S (2001) Left–right positioning of the adult rudiment in sea urchin larvae is directed by the right side. Development 128:4935–4948

Akasaka K, Uemoto H, Wilt F, Mitsunaga-Nakatsubo K, Shimada H (1997) Oral–aboral ectoderm differentiation of sea urchin embryos is disrupted in response to calcium ionophore. Dev Growth Differ 39:373–379

Amemiya S (1996) Complete regulation of developmental throughout metamorphosis of sea urchin embryos devoid of macromeres. Dev Growth Differ 38:465–476

Arenas-Mena C, Cameron AR, Davidson EH (2000) Spatial expression of Hox cluster genes in the ontogeny of a sea urchin. Development 127:4631–4643

Asano S, Yoshida A, Yashiro H, Kobayashi Y, Morisato A, Ogawa H, Takeguchi N, Morii M (2004) The cavity structure for docking the K^+-competitive inhibitors in the gastric proton pump. J Biol Chem 279:13968–13975

Boorman CJ, Shimeld SM (2002) The evolution of left–right asymmetry in chordates. Bioessays 24:1004–1011

Coffman JA, Davidson EH (2001) Oral–aboral axis specification in the sea urchin embryo. I. Axis entrainment by respiratory asymmetry. Dev Biol 230:18–28

Coffman JA, McCarthy JJ, Dickey-Sims C, Robertson AJ (2004) Oral–aboral axis specification in the sea urchin embryo II. Mitochondrial distribution and redox state contribute to establishing polarity in *Strongylocentrotus purpuratus*. Dev Biol 273:160–171

Cooke J (2004) The evolutionary origins and significance of vertebrate left–right organisation. Bioessays 26:413–421

Davidson JS, Baumgarten IM (1988) Glycyrrhetinic acid derivatives: a novel class of inhibitors of gap-junctional intercellular communication. Structure–activity relationships. J Pharmacol Exp Ther 246:1104–1107

Duboc V, Rottinger E, Besnardeau L, Lepage T (2004) Nodal and BMP2/4 signaling organizes the oral–aboral axis of the sea urchin embryo. Dev Cell 6:397–410

Duboc V, Röttinger E, Lapraz F, Besnardeau L, Lepage T (2005) Left–right asymmetry in the sea urchin embryo is regulated by Nodal signaling on the right side. Dev Cell 9:147–158

DuVall MD, Zhu S, Fuller CM, Matalon S (1998) Peroxynitrite inhibits amiloride-sensitive Na^+ currents in *Xenopus* oocytes expressing $\alpha\beta\gamma$-rENaC. Am J Physiol 274:C1417–C1423

Fujiwara A, Kamata Y, Kamamoto M, Hino A, Mizoguchi H, Yasumasu I (1997) Abnormal embryos of sea urchin induced by A23187. Zool Sci 14:76

Gambino R, Romancino DP, Cervello M, Vizzini A, Isola MG, Virruso L, Di Carlo M (1997) Spatial distribution of collagen type I mRNA in *Paracentrotus lividus* eggs and embryos. Biochem Biophys Res Commun 238:334–337

Hamada H, Meno C, Watanabe D, Saijoh Y (2002) Establishment of vertebrate left–right asymmetry. Nat Rev Genet 3:103–113

Hamada M, Kiyomoto M (2003) Signals from primary mesenchyme cells regulate endoderm differentiation in the sea urchin embryo. Dev Growth Differ 45:339–350

Harris C, Fliegel L (1999) Amiloride and the Na^+/H^+ exchanger protein: mechanism and significance of inhibition of the Na^+/H^+ exchanger (review). Int J Mol Med 3:315–321

Ishii Y, Hibino T, Nishino A, Levin M, Amemiya S (2003) An inhibitor for H^+/K^+-ATPase disrupted the left–right asymmetry in the echinoid embryo. Zool Sci 20:1552

Jiang S, Meadows J, Anderson SA, Mukkada AJ (2002) Antileishmanial activity of the antiulcer agent omeprazole. Antimicrob Agents Chemother 46:2569–2574

Kramer-Zucker AG, Olale F, Haycraft CJ, Yoder BK, Schier AF, Drummond IA (2005) Cilia-driven fluid flow in the zebrafish pronephros, brain and Kupffer's vesicle is required for normal organogenesis. Development 132:1907–1921

Landry DW, Reitman M, Cragoe EJ Jr, Al-Awqati Q (1987) Epithelial chloride channel. Development of inhibitory ligands. J Gen Physiol 90:779–798

Levin M (2003) Motor protein control of ion flux is an early step in embryonic left–right asymmetry. Bioessays 25:1002–1010

Levin M (2004a) The embryonic origins of left–right asymmetry. Crit Rev Oral Biol Med 15:197–206

Levin M (2004b) A novel immunohistochemical method for evaluation of antibody specificity and detection of labile targets in biological tissue. J Biochem Biophys Methods 58:85–96

Levin M (2005) Left–right asymmetry in embryonic development: a comprehensive review. Mech Dev 122:3–25

Levin M, Nascone N (1997) Two molecular models of initial left–right asymmetry generation. Med Hypotheses 49:429–435

Levin M, Thorlin T, Robinson KR, Nogi T, Mercola M (2002) Asymmetries in H^+/K^+-ATPase and cell membrane potentials comprise a very early step in left–right patterning. Cell 111: 77–89

Logan CY, Miller JR, Ferkowicz MJ, McClay DR (1999) Nuclear β-catenin is required to specify vegetal cell fates in the sea urchin embryo. Development 126:345–357

McGrath J, Somlo S, Makova S, Tian X, Brueckner M (2003) Two populations of node monocilia initiate left–right asymmetry in the mouse. Cell 114:61–73

Mercola M (2003) Left–right asymmetry: nodal points. J Cell Sci 116:3251–3257

Mitsunaga K, Fujino Y, Yasumasu I (1987) Distributions of H^+,K^+-ATPase and Cl^-, HCO^{3-}-ATPase in micromere-derived cells of sea urchin embryos. Differentiation 35:190–196

Mukherjee T, Mandal D, Bhaduri A (2001) Leishmania plasma membrane Mg^{2+}-ATPase is a H^+/K^+-antiporter involved in glucose symport. Studies with sealed ghosts and vesicles of opposite polarity. J Biol Chem 276:5563–5569

Munson KB, Lambrecht N, Sachs G (2000) Effects of mutations in M4 of the gastric H^+,K^+-ATPase on inhibition kinetics of SCH28080. Biochemistry 39:2997–3004

Møller JV, Juul B, le Maire M (1996) Structural organization, ion transport, and energy transduction of P-type ATPases. Biochim Biophys Acta 1286:1–51

Nathan RD, Kanai K, Clark RB, Giles W (1988) Selective block of calcium current by lanthanum in single bullfrog atrial cells. J Gen Physiol 91:549–572

Nonaka S, Shiratori H, Saijoh Y, Hamada H (2002) Determination of left–right patterning of the mouse embryo by artificial nodal flow. Nature 418:96–99

Nonaka S, Tanaka Y, Okada Y, Takeda S, Harada A, Kanai Y, Kido M, Hirokawa N (1998) Randomization of left–right asymmetry due to loss of nodal cilia generating leftward flow of extraembryonic fluid in mice lacking KIF3B motor protein. Cell 95:829–837

Okada Y, Takeda S, Tanaka Y, Izpisua Belmonte JC, Hirokawa N (2005) Mechanism of nodal flow: a conserved symmetry breaking event in left–right axis determination. Cell 121: 633–644

Peterson KJ, Cameron RA, Davidson EH (2000) Bilaterian origins: significance of new experimental observations. Dev Biol 219:1–17

Ransick A, Rast JP, Minokawa T, Calestani C, Davidson EH (2002) New early zygotic regulators expressed in endomesoderm of sea urchin embryos discovered by differential array hybridization. Dev Biol 246:132–147

Raya A, Kawakami Y, Rodriguez-Esteban C, Ibanes M, Rasskin-Gutman D, Rodriguez-Leon J, Buscher D, Feijo JA, Izpisua Belmonte JC (2004) Notch activity acts as a sensor for extracellular calcium during vertebrate left–right determination. Nature 427:121–128

Ryan AK, Blumberg B, Rodriguez-Esteban C, Yonei-Tamura S, Tamura K, Tsukui T, de la Pena J, Sabbagh W, Greenwald J, Choe S, Norris DP, Robertson EJ, Evans RM, Rosenfeld MG, Izpisua Belmonte JC (1998) Pitx2 determines left–right asymmetry of internal organs in vertebrates. Nature 394:545–551

Sachs G, Shin JM, Briving C, Wallmark B, Hersey S (1995) The pharmacology of the gastric acid pump: the H^+,K^+ ATPase. Annu Rev Pharmacol Toxicol 35:277–305

Sanders SW, Tolman KG, Greski PA, Jennings DE, Hoyos PA, Page JG (1992) The effects of lansoprazole, a new H^+,K^+-ATPase inhibitor, on gastric pH and serum gastrin. Aliment Pharmacol Ther 6:359–372

Showman RM, Foerder CA (1979) Removal of the fertilization membrane of sea urchin embryos employing aminotriazole. Exp Cell Res 120:253–255

Tanaka Y, Okada Y, Hirokawa N (2005) FGF-induced vesicular release of Sonic hedgehog and retinoic acid in leftward nodal flow is critical for left–right determination. Nature 435: 172–177

Toyoizumi R, Kobayashi T, Kikukawa A, Oba J, Takeuchi S (1997) Adrenergic neurotransmitters and calcium ionophore-induced situs inversus viscerum in *Xenopus laevis* embryos. Dev Growth Differ 39:505–514

Vakil N (2003) Review article: esomeprazole, 40 mg once daily, compared with lansoprazole, 30 mg once daily, in healing and symptom resolution of erosive oesophagitis. Aliment Pharmacol Ther 17(Suppl 1):21–23

Vlahou A, Gonzalez-Rimbau M, Flytzanis CN (1996) Maternal mRNA encoding the orphan steroid receptor SpCOUP-TF is localized in sea urchin eggs. Development 122:521–526

Weitzel HE, Illies MR, Byrum CA, Xu R, Wikramanayake AH, Ettensohn CA (2004) Differential stability of β-catenin along the animal–vegetal axis of the sea urchin embryo mediated by dishevelled. Development 131:2947–2956